Magnetic nanocomposites for organic compatible miniaturized antennas and inductors

P. Markondeya Raj[+], Prathap Muthana, T. Danny Xiao*, Lixi Wan, Devarajan Balaraman, Isaac Robin Abothu, Swapan Bhattacharya, Madhavan Swaminathan and Rao Tummala

Packaging Research Center
813 Ferst Drive NW
Georgia Institute of Technology
Atlanta GA 30332-0560
+ raj@ece.gatech.edu Phone: 404 894 2652 Fax: 404 894 3842
* Inframat Corporation, 74 Batterson Park Road, Farmington, Connecticut 06032

Abstract: **Current wireless systems are limited by RF technologies in their size, communication range, efficiency and cost. RF circuits are difficult to miniaturize without compromising performance. Antennas and inductors are major impediments for system miniaturization because of the lack of magnetic materials with suitable high frequency properties. Keeping antenna and inductor requirements into consideration, two magnetic nanocomposite systems – silica coated cobalt-BCB and Ni ferrite-epoxy were investigated as candidate materials. Nanocomposite thick film structures (125-225 microns) were screen printed onto organic substrates. Parallel plate capacitors and single coil coplanar inductors were fabricated on these films to characterize the electrical and magnetic properties of these materials at low and high frequencies. Electrical characterization showed that the Co/SiO_2 nanocomposite sample has a permeability and a matching permittivity of ~10 at GHz frequency range making it a good antenna candidate. Both polymer matrix composites retain high permeability at 1-2 GHz.**

I. INTRODUCTION

Recent developments in IC and system-level packaging technologies have lead towards smaller RF transceivers with embedded passive components. Amongst the RF components, antenna is still considered a major barrier for system miniaturization. The effectiveness of conversion of electrical power to electromagnetic power becomes practical only when the antenna size becomes larger than an appreciable fraction of the wave length. Low profile antennas suffer from relatively narrow bandwidth, substrate dielectric loss, mutual coupling with their substrate and surface wave perturbation issues. If the material surrounding the antenna has high-permittivity and permeability, the wavelength (λ) in such material will be shorter by a factor of $1/\sqrt{\varepsilon\mu}$. Therefore, magnetic nanocomposites can potentially lead to an order of magnitude reduction in size because of their combined effect of high permittivity and permeability. These dielectrics can increase the path of the normal current and hence the radiation efficiency. By tuning the nanocomposite formulation, the material can be designed to have equal permittivity and permeability in order to have good impedance match with that of free space. The bandwidth of antennas on magnetic substrate are also known to be wider than those on conventional dielectric substrate. In this work, novel magnetic nanocomposites were synthesized and investigated for their magnetic permeability, dielectric constant and dielectric loss.

Reducing the particle size and the separation between neighboring particles down to the nanoscale leads to novel magnetic coupling phenomena resulting in higher permeability and lower magnetic anisotropy. Co- or Fe-based nanocomposites show much higher permeability than those obtainable from the bulk Co or Fe metal. This large enhancement in permeability is due to the interparticle exchange coupling effect. The exchange interaction, which leads to magnetic ordering within a grain, extends out to neighboring environments (through either a spin polarization or super-exchange interaction mechanism) within a characteristic distance, l_{ex}. For Fe or Co, l_{ex} is 30 nm. The exchange interaction in nanocomposites also leads to a cancellation of magnetic anisotropy of individual particles and the demagnetizing effect, leading to ultrasuperior soft magnetic properties. By choosing a system with high tunneling excitation energy, a huge increase in the resistivity (from 10^{-6} Ohm-cm in pure metal to 10^{9} Ohm-cm in nanocomposite) can be achieved through the nanocompositing technique. Because of the nanosized metal particles, the eddy currents produced within the particle are also negligibly small, leading to much lower loss for nanocomposites compared to that of conventional microsized ferrites and powder materials. Similarly, nanosized Ni ferrite particles are also expected to have superior properties compared to their microsized counter parts.

It is well known that most high permeability and high permittivity materials have frequency-dependent properties. This makes it difficult to design using these otherwise high-performance materials. Hence, there is a strong interest to

0-7803-9085-7/05/$20.00 ©2005 IEEE

characterize the high-frequency properties of these materials. Our previous work reported high frequency properties of thin barium titanate, strontium titanate films and carbon black – epoxy nanocomposites using multiline calibration method with Coplanar Wave Guide structures [1]. Previous studies by Zhang et al. [2] reported that while bulk Ni ferrite has unstable magnetic permeability beyond 100 MHz, the Co-silica system shows stable permeability till 240 MHz. In this work, Ni ferrite-epoxy and Co-Silica/BCB systems were investigated with parallel plate capacitor and inductor structures, for their properties till 2 GHz. Based on these measurements, the suitability of these materials for high frequency antenna and inductor applications will be assessed.

II. SYNTHESIS AND FABRICATION

A. *Silica-coated Co Synthesis*: Inframat's technology for the synthesis and processing of magnetic nanocomposite is different from the conventional metallic and ferrite materials. The Co/SiO_2 nanocomposie was synthesized using an aqueous solution reaction technique, which is capable of synthesizing a variety of nanostructured materials including metal, oxides, and composites in large quantities. In the synthesis of Co/SiO_2 magnetic nanocomposite powders, experimental procedures include preparing the starting precursors containing Co and SiO_2, co-atomization of the precursors to form colloidal solution of Co and SiO_2 and annealing the colloidal solution to form Co/SiO_2 nanocomposite powders.

A typical TEM bright field image for Inframat's synthetic Co/SiO_2 nanocomposite is shown in Fig. 1. The TEM studies revealed that the synthetic nanocomposite is a two-phase material, where nanoparticles of Co are coated with a thin film of silica. The Co phase has an average particle size of ~30 nm. Selected area electron diffraction experiments indicated that the Co particles are fcc nanocrystals, where the matrix silica phase is amorphous.

In order to study the microstructure in detail at the nanometer level, localized regions at the Co/silica interface have been studied using a microbeam diffraction technique. The diffraction beam was reduced to approximately 10 nm in size and diffracted at the area of interest. Two phases were found in localized regions, including fcc Co and γ-phase SiO_2. Majority SiO_2 coating is amorphous, as indicated in the XRD and other selected large area diffraction techniques.

The Co-Silica nanoparticles (50 wt.% each) were mixed with Benzo Cyclo Butene (BCB) polymer (Dow Chemicals, Midland, Michigan) using conventional mixing. The as-received BCB 3022-46 has 46 % volatile mesitylene. A paste (60 wt. % inorganic and 40 wt. % as received polymer) with suitable viscosity was then screen printed to a thickness of 225 microns onto high-temperature copper-clad FR-4 substrates that are compatible with BCB curing at 250 C. Copper is sputtered to a thickness of 3 microns, and patterned by an etch-back process to form the top electrode.

B. Ferrite synthesis: In the ferrite nanoparticles synthesis, again, a low temperature synthesis approach based on the aqueous synthesis method has been developed to synthesis very fine $(Ni_{0.5}Zn_{0.5})Fe_2O_4$ nanoparticles. The procedures include (1) preparation of a salt solution that contains Ni, Zn, and Fe with the selected atomic ratio, (2) addition of the NH_4OH solution into the Ni and Fe precursor solution to adjust pH, without any precipitation, (3) conversion of the precursor solution into a Ni-Fe-O complex powder, and (4), conversion (calcine) of the Ni-Zn-Fe-O material into nanostructured $(Ni_{0.5}Zn_{0.5})Fe_2O_4$ at low temperature in hydrogen and oxygen controlled atmosphere.

In the microstructure studies, HRTEM specimens were prepared by dispersing the powders in methanol. Drops of this solution were then deposited on a carbon-grit and observed in the microscope. Bright field images, electron diffraction, and lattice images were carried out. A typical HRTEM atomic resolution image shown the morphologies of the ferrite nanoparticle materials is illustrated in Fig. 1. TEM studies at atomic resolution and electron diffraction reveal that the synthetic $(NiZn)Fe_2O_4$ nanoparticle is hexagonal. The size of the ferrite nanoparticle is ~ 5 to 15 nm.

The nanoparticles of ferrite were dispersed into a commercial epoxy to form a thick paste. The paste is then screen-printed onto a FR4 substrate to a thickness of 125 microns. The composition of the paste consists of 50-70% nanoparticles uniformly dispersed in an epoxy resin. The epoxy can be cured to form a dense solid at temperatures between 80-140^oC. The curing time correspondingly varies from 5 hrs to 30 minutes. In this study, the films were cured at 140 C for 30 minutes. The top electrode was sputtered to a thickness of 3 microns and patterned by an etch-back process.

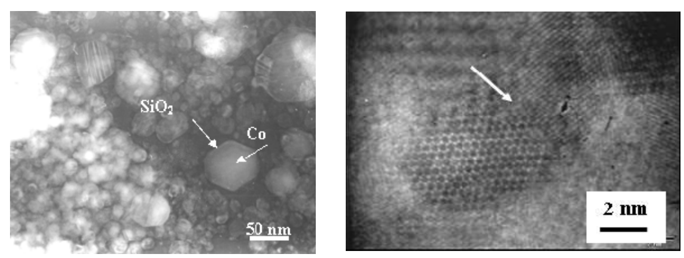

Fig 1. A typical TEM micrograph shows a two phase material, where amophous SiO_2 films are coated on the surface of Co nanocrystals. A typical atomic resolution TEM micrograph showing the microstructure of the $(NiZn)Fe_2O_4$ nanoparticles Arrow points to the boundary between two nanoparticles.

III. ELECTRICAL CHARACTERIZATION

Parallel plate capacitor and single coil inductor structures were fabricated to characterize the electrical properties of these materials. The structure details are described in Fig. 2. Different sized components were used to check the consistency in the measurements and also for internal calibration. To characterize the permittivity, both high frequency and low frequency characterization techniques were employed. Low frequency characteristics were measured with a Precision LCR meter (Agilent 4285A). The dielectric constants of both the nanocomposites are much higher than the base polymer employed. The observed decrease in dielectric constant with frequency (Fig. 3) in metal-insulator composites is indicative of the interfacial polarization relaxation.

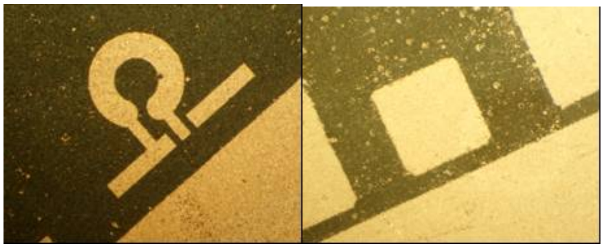

Fig. 2. Fabricated inductor and capacitor structures. The outer diameter for the inductor coil is 1.22 mm while the inner diameter is 0.53 mm. The size of the capacitor is 2.33x 2.33 mm. For the capacitor, the adjacent metal is connected to the bottom electrode.

The high frequency measurements were conducted with an s-parameter Network Analyzer (HP Model 8720 ES). Two-port measurements were employed to eliminate any systematic errors that occur with single port measurements. The probes were ground-signal type with a spacing of 500 microns. Ground-Signal-Ground probes were not used in this study. The transfer impedance (Z_{12} or Z_{21}) can be estimated from the s-parameters as:

$$Z = 50\frac{2S_{12}}{(1-S_{11})(1-S_{22})-S_{12}S_{21}} \qquad (1)$$

for 2-port measurement with two probes located on the same position of a coupon. Another form of this relationship is also reported in the literature [3].

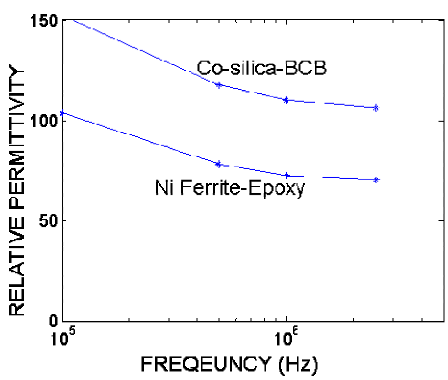

Fig. 3. Low frequency permittivity measurements of magnetic nanocomposites.

A. Equations for parallel plate capacitor: Different size of capacitors built on the same substrate, using same material and processing can be used for internal calibration. Below the first self-resonant frequency, a capacitor can be deemed equivalent to a capacitor, inductor and resistor connected in series. The equation for the serial circuit can be expressed as:

$$Z = j\omega L + \frac{1}{j\omega C} + R \qquad (2)$$

where Z is the impedance of the equivalent circuit. L, C, and R are inductance, capacitance and resistance of the circuit respectively. ω is the angular frequency. L, C, and R are functions of frequency. Since there are three unknowns in the equation different size capacitors would be needed. The goal of this work is to extract permeability and permittivity. The equations for the two capacitors will be:

$$\mathrm{Im}(Z_1) = j\omega L_1 + \frac{1}{j\omega C_1} \qquad (3)$$

$$\mathrm{Im}(Z_2) = j\omega L_2 + \frac{1}{j\omega C_2} \qquad (4)$$

The geometric part of the capacitance, C_o, for parallel plate capacitor can be estimated using as $\varepsilon_0 \frac{A}{d}$ where A is the area of the plane and d is the distance of separation between the planes. There is no simple equation for the inductance. Generally, inductance with frequency dependent material can be expressed as: $L = \mu(f)L_0$ where L_0 is the inductance of an inductor filled with a non-magnetic material. The L_0 value can be estimated from the above equations by plugging in the permittivity and permeability measurements done independently at 50-100 MHz using bulk inductors at Inframat Corporation [2]. Using the estimated L_0 and C_0, the permeability and permittivity at all the other frequencies can be solved from the simultaneous equations (3-4) for two capacitors. Figs. 4 and 5 show the permittivity and permeability values for both the nanocomposite systems. It is interesting to note that both materials retain a permittivity of more than 10 at GHz frequency. The permeability value for Co-Silica-BCB is close to 10 at 1 GHz frequency as seen in Fig. 5.

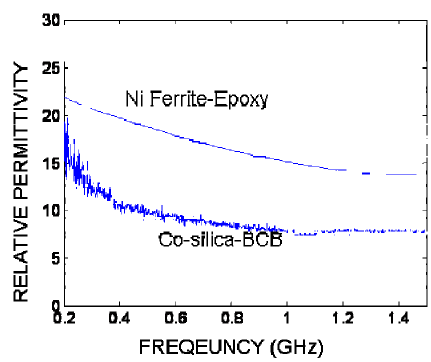

Fig. 4. High frequency permittivity of magnetic nanocomposites.

B. Estimation of Ni Ferrite permeability from inductor structures: Different size inductors were built on the magnetic nanocomposite substrate as well as a glass microslide with known permability of 1 and same thickness as the magnetic nanocomposite (125 microns). For the nanocomposite sample, the inductor is completely buried by screen printing the paste above and below the structure, while opening the pads for testing. Using same inductor structures on glass and nanocomposite, the permeability was directly estimated from the impedance measurements as:

$$\mu = \frac{\mathrm{Im}(Z)_{Nanocomposite}}{\mathrm{Im}(Z)_{Glass}} \qquad (5)$$

It should be noted that the actual equivalent circuit of the test structure is much more complicated, with an inductor and resistor in series, and a capacitor in parallel. The resistive effects, amplified by the loss, and capacitive effects, amplified by the high permittivity nanocomposite, significantly affect this estimate. Hence, this analysis is not suitable for higher frequencies, where the Im(Z) Vs frequency deviates from a straight line. The obtained inductance as a function of frequency is plotted in Fig. 5, along with that of Co-Silica-BCB for comparison. The measurement indicates that the ceramic-polymer composite retains a permeability of 2.5 at 1 GHz frequency.

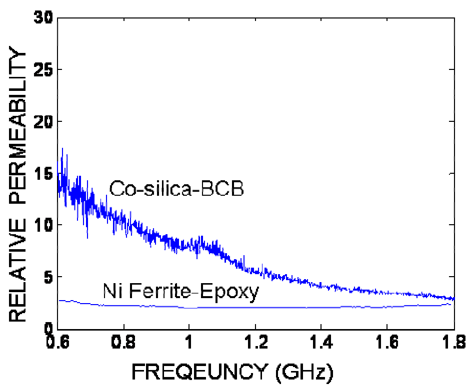

Fig. 5. High frequency permeability of magnetic nanocomposites.

High frequency characteristics of metal-based magnetic nanocomposites were previously reported by Miura et al [4]. In their work, iron powder resin showed a permeability decreasing from 3 to 2, as the frequency increases from 1 GHz to 5 GHz. Similarly, $Ba_2Ni_2Fe_{12}O_{22}$ showed a steep decrease in permeability from 4.5 at 200 MHz to 2 at 1 GHz, as studied by Shin and Oh [5]. While the permeabilities of $Fe_{72}Al_{11}O_{17}$ and $Fe_{55}Al_{18}O_7$ are not stable beyond 1 GHz, $Co_{59}Zr_{12}O_{30}$ showed stable properties of 70-80 beyond 1 GHz. These are presumably not organic compatible materials. Polymer based composites showed a steep decrease in permeability from 10 at 1GHz to 1 at 3 GHz, as reported by Yoshida et al [6]. The Co-Silica-Polymer system showed higher permeability and permittivity than the polymeric magnetic nanocomposite systems reported in the literature because of its nanoparticle size and silica coating. The high frequency stability of the Ni ferrite permeability is always of concern, as is also seen in this study. The nanocrystalline Ni ferrite is expected to yield higher permeabilities than their bulk counterparts. One reason this was not observed in these studies could be the use of lossy polymer such as epoxy which could alter the inductive behavior considerably. High performance BCB is currently being used as the nanocomposite matrix to gain further improvement in properties.

The dielectric loss of Co-silica-BCB varied with the filler content. Incorporation of metal inside a polymer increases the dielectric loss. In the nanocomposites studied here, the silica coating is expected to prevent the charge leakage and help lower the losses. The low frequency dielectric loss of these nanocomposites varied from 0.003 for low filler content to 0.08 for higher filler content. Further improvements in the formulation and dispersion methodologies are now being investigated to lower the loss at high filler contents.

IV. CONCLUSIONS

Thick film Ni ferrite-epoxy and Co-silica-BCB nanocomposites were characterized for their permittivity and permeability over broad frequency range to assess their suitability for antenna and inductor applications. Interestingly, both materials show high permittivity and permeability. Co-silica-BCB shows matching permittivity and permeability of 5-10 making it a good candidate for miniaturized antennas. Fabricated inductor structures on Ni ferrite-epoxy showed that the material retains a permeability of 2.5-3 at GHz frequency range. Both material systems show significant advances over existing organic (Printed Wiring Board) compatible magnetic nanocomposites for high-frequency inductor applications.

ACKNOWLEDGMENT

This work was supported by the National Science Foundation (NSF) through the NSF ERC in Electronic Packaging (EEC-9402723) at Georgia Institute of Technology. The authors also than Venky Sundaram (PRC, Georgia Tech.) and Yong Kyu Yoon (ECE, Georgia Tech.) for their assistance. Dr. T. Danny Xiao thanks Inframat Corp. for funding his research activities in conducting this work.

REFERENCES

[1] D. Balarman, P. M. Raj et al., " BaTiO3 films by low-temperature hydrothermal techniques for next-generation packaging applications", *Journal of Electroceramics*, 13, 95-100, 204.

[2] Y. D. Zhang, S. H. Wang, D. T. Xiao, J. I. Budnick and W. A. Hines, "Nanocomposite Co/SiO2 soft magnetic nanomaterials", *IEEE Trans. Magnetics*, Vol. 37, no. 4, July 2001, pp. 2275-2277.

[3] Istvan Novak, Jason R Miller, "Frequency – Dependent Characterization of Bulk and Ceramic Bypass Capacitors", Poster material for the *12th Topical Meeting on Electrical Performance of Electronic Packaging*, October 2003, Princeton, NJ.

[4] T. Miura and S. Nakagawa, "Spectrum management of pulse transmission by high-cut filter using magnetic loss", *IEEE International Microwave Symposium, Phoenix*, June 2001, Digest vol. 1, pp. 463-466.

[5] J. Y. Shin and J. H. Oh, "The microwave absorbing phenomena of ferrite absorbers", *IEEE Trans. Magnetics*, vol. 29, no. 6, Nov. 1993, pp. 3437-3439.

[6] S. Yoshida et al., "High-frequency noise suppression in downsized circuits using magnetic granular films", *IEEE Trans. Magnetics*, vol. 37, no. 4, July 2001, pp. 2401-2403.